

PT-Symmetric potential impact on the scattering of a Bose-Einstein condensate from a Gaussian Obstacle

Jameel Hussain,¹ Muhammad Nouman,² Farhan Saif,¹ and Javed Akram^{2,*}

¹*Department of Electronics, Quaid-i-Azam University, Islamabad, 45320 Pakistan*

²*Department of Physics, COMSATS University Islamabad, Pakistan*

(Dated: November 3, 2022)

The scattering of a Bose-Einstein Condensate (BEC) from a Gaussian well and Gaussian barrier is investigated over a wide range of depths and heights, respectively. We compare analytical and numerical results for a BEC scattering from Gaussian Obstacles, both in the presence and in the absence of *PT*-symmetric potential. And we find out that the Complex Ginzburg-Landau Equation (CGLE) method has limitations due to the limited number of variational parameters of the ansatz. We also find that the presence of the *PT*-symmetric potential controls the reflection and the transmission flux of the BEC through the Gaussian Obstacle.

I. INTRODUCTION

The theoretical and experimental realization of Bose-Einstein Condensate (BEC) created many new possibilities to observe and analyze the quantum phenomena on macroscopic level [1–3]. Moreover, the confinement of the BEC in different potential traps systems provide us better control over BEC [4], for instance, to study interference [5], solitons creation [6–8], scattering [9–11] tunneling [12] and interaction of impurities with the BEC [13, 14].

In 1998 Bender and Boettcher presented the idea that some non-Hermitian Hamiltonians can have real spectrum [15]. Such Hamiltonians, with complex potentials follow the *PT*-symmetry, mathematically ensured by the condition $V(x) = V^*(-x)$, where $V(x)$ represents the external potential of the system. Bender and Boettcher idea is an extension to quantum mechanics from the real to the complex domain. *PT*-symmetric extension of quantum mechanics for non-hermitian Hamiltonian helps to encapsulate the idea of loss and gain in the system [16–18]. The *PT*-symmetry has been manipulated and realized experimentally in optics [17, 19], and later on it is extended for the BEC [20, 21].

In this paper, we consider the BEC scattering from the Gaussian well and Gaussian barrier in the absence of (conservative system), and in the presence of (non-conservative) *PT*-symmetric environment. For such a non-conservative *PT*-Symmetric system, in a double-well potential well, the atoms can be injected from one side and removed from the other side simultaneously [22], the injection and removal of atoms can be done by using laser radiation [23, 24], the atom can be loaded at the desired side of the double well potential to ensure the exact compensation by atomic lasers [25–27]. We study analytically and numerically quasi-one-dimensional (1D) scattering dynamics of a BEC, the scattering includes both transmission and reflection from a Gaussian barrier. We study that the transmission and reflection can be controlled by the barrier height V_0 . The *PT*-symmetric potential introduce another parameter to control the scattering characteristics of a BEC at the Gaussian barrier in the harmonic potential. In this respect, we organize this paper as follows. We discuss the theoretical model in Sec. II. A comparison of analytical and numerical results is given in Sec. III. In Sec. IV, we present the scattering of a BEC from a repulsive barrier in the absence of *PT*-symmetric potential. Later, in Sec. V, we study the impact of *PT*-symmetric potential on the scattering of a BEC from a repulsive Gaussian barrier. The summary and conclusion is discussed in Sec. VI and the last Sec. VII is assigned for acknowledgment.

II. THEORETICAL MODEL

The BEC dynamics in a quasi-1D regime is governed by the quasi-1D GPE, [28–31]

$$i\hbar \frac{\partial \psi(x,t)}{\partial t} = \left[-\frac{\hbar^2}{2m} \frac{\partial^2}{\partial x^2} + V(x) + g_s |\psi(x,t)|^2 \right] \psi(x,t), \quad (1)$$

with the normalization condition $\int |\psi(x,t)|^2 dx = 1$. Here $\psi(x,t)$ describes the wavefunction of the condensate, m represents mass of individual atom, t defines time and the x stands for a 1D-space coordinate. The BEC experiences external potential $V(x) = V_h + V_g + W(x)$, with V_h denotes the harmonic potential, V_g illustrates the Gaussian potential barrier, and $W(x)$ stands for the complex *PT*-symmetric potential. The interaction strength can be described as $g_s = 2N\hbar\omega_r a_s$, where a_s represents the s-wave scattering length [13], N stands for the number of atoms in the BEC

and ω_r characterizes the radial frequency component of the trap [7]. To do numerical simulation, we make 1D-GPE (1) dimensionless. Therefore, we measure time in ω_x^{-1} , length of the harmonic oscillator along x-axis in $\sqrt{\hbar/m\omega_x}$ and energy in $\hbar\omega_x$. The quasi-1D GPE reduce to the dimensionless form,

$$i\frac{\partial\psi(x,t)}{\partial t} = \left[-\frac{1}{2}\frac{\partial^2}{\partial x^2} + V(x) + g_s|\psi|^2 \right] \psi(x,t), \quad (2)$$

with dimensionless interaction strength reduce to $g_s = 2N\omega_r a_s/(\omega_x L)$, here $L = \sqrt{\hbar/m\omega_x}$ denotes the length of the oscillator along x-axis and the dimensionless external potential is given by,

$$V = \frac{x^2}{2} + V_0.e^{-x^2} + i.W_0.x.e^{-x^2}, \quad (3)$$

here, V_0 defines the dimensionless Gaussian well depth ($V_0 < 0$) and Gaussian barrier height ($V_0 > 0$). While, the gain ($W_0 > 0$) and the loss ($W_0 < 0$) of the BEC atoms can be controlled by the strength of PT -symmetric potential W_0 . In this paper, we do not study the impact of the width of the Gaussian obstacle on the dynamics of the BEC, therefore we chosen a constant width "1". However, according to our understanding, the width controls the tunneling between the adjacent wells, which needs a detailed investigation.

A. Analytical method

The variational approach gives the analytical information about the numerical solution of the system [32, 33]. Here in this paper, we investigate the analytical method to compare and validate our numerical simulations results. Additionally, we want to explore the limitations of the analytical technique. The analytical method relies on the choice of the initial normalized trial wave-function. Here, we let the initial normalized ansatz as

$$\psi(x,t) = \frac{1}{\sqrt{a(t)}\sqrt{\pi}} e^{-\frac{(x-x_0(t))^2}{2a(t)^2} + ix\alpha(t) + ix^2\beta(t)}, \quad (4)$$

where $x_0(t)$ represents the mean position of the BEC. Here $a(t)$ defines the dimensionless width of the BEC, $\alpha(t)$ represents the velocity of the BEC and $\beta(t)$ represents the time-dependent derivative of the width of the BEC. To study our system analytically, we take the Lagrangian density as,

$$\mathcal{L} = \frac{i}{2} \left(\psi \frac{\partial\psi^*}{\partial t} - \psi^* \frac{\partial\psi}{\partial t} \right) - \frac{1}{2} \left| \frac{\partial\psi}{\partial x} \right|^2 + V(x)|\psi|^2 + \frac{g_s}{2} |\psi|^4. \quad (5)$$

By using above Lagrangian density, we get the Lagrangian of the system $L = \int \mathcal{L} dx$. We begin by writing the total Lagrangian of the system as a sum of two terms, i.e., $L = L_c + L_{nc}$ where L_c represents the conservative term and L_{nc} describes the non-conservative part of the Lagrangian. Here, the conservative system means the potential without complex part of the external potential while non-conservative term represents the complex part of the external potential. By using the above Lagrangian, we determine the complex Ginzburg-Landau equation (CGLE) as [34–37],

$$\frac{d}{dt} \left(\frac{\partial L_c}{\partial \dot{q}} \right) - \frac{\partial L_c}{\partial q} = 2Re \left[\int_{-\infty}^{\infty} W(x)\psi \frac{\partial\psi^*}{\partial q} dx \right], \quad (6)$$

where q stands for variational parameters $a(t)$, $x_0(t)$, $\alpha(t)$ and $\beta(t)$. By using Eq. (5) and Eq. (6), we calculate the time-dependent equation for the mean position of the BEC,

$$x_0''(t) + x_0(t) = \frac{2V_0 x_0(t)}{\xi(t)^{\frac{3}{2}}} e^{-\frac{x_0^2(t)}{\xi(t)}}, \quad (7)$$

where $\xi(t) = 1 + a^2(t)$, here, we ignore the non-conservative term, however, we give the detailed non-conservative equation in appendix A. The dimensionless width of the BEC changes with time as it collides with the Gaussian barrier. To understand this phenomenon, we determine analytically the dimensionless time-dependent equation for the width of the BEC as,

$$a''(t) + a(t) = \frac{1}{a^3(t)} + \frac{g_s}{\sqrt{2\pi}a^2(t)} + \frac{2V_0 a(t)}{\xi(t)^{\frac{3}{2}}} e^{-x_0^2(t)/\xi(t)} \left[1 - \frac{2x_0^2(t)}{\xi(t)} \right], \quad (8)$$

while deriving above Eq. (8) again we neglect the complex part of the potential, L_{nc} . "Non-conservative" L_{nc} part makes our equations cumbersome, therefore that equation is presented in appendix A.

B. Numerical method

To numerically simulate our research problem, we perform discretization of the dimensionless quasi-1D GPE Eq. (2). We take space-step as $\Delta x = 0.0177$ and we choose the time step as $\Delta t = 0.0001$. Here, we use the time-splitting spectral method [38–43]. To get the numerical equilibrium results for the shifted harmonic potential $V = (x - 35)^2/2$, we use strange-split method, where the ground state wavefunction for different interaction strength is achieved by simulating in imaginary-time $\tau = it$. For the dynamical evolution of the wavefunction of the BEC, it is worthwhile to mention that the ground state wavefunction serves as an initial condition for the rest of the numerical simulations.

III. A COMPARISON OF ANALYTICAL AND NUMERICAL RESULTS

To study the limitation of analytical results as discussed in Sec. II A, we compare them with numerical results produced in Sec. II B. The comparison of analytical and numerical results are presented in Fig. (1-4) for attractive Gaussian well and for a repulsive Gaussian barrier. In order to understand the basic scattering behavior, we choose the dimensionless interaction strength as $g_s = 30$. To compare analytical and numerical results, for attractive Gaussian well, we plot the temporal density graph in the absence of PT -symmetry in Fig. 1(a-b) and in Fig. 2(a-b) for a dimensionless Gaussian well depth $V_0 = -500$, and $V_0 = -1000$ respectively. Similarly, in Fig. 1(c-d) and in Fig. 2(c-d), we present the numerical and analytical results for the scattering of a BEC in the presence of PT -symmetry environment for the same dimensionless interaction strength and well depths as mentioned above. Initially, we place a BEC in this potential $V = (x - 35)^2/2$. Later, the BEC set into motion by quenching the trapping potential minima to coincide with the maxima of the Gaussian barrier as $V = x^2/2 + V_0 e^{-x^2}$. To analyze our results, we divide our research problem into three different subsections, for attractive Gaussian well, low repulsive Gaussian barrier and high repulsive Gaussian barrier.

A. Attractive Gaussian well

The BEC initially placed at $x_0 = 35$, later at time $t = 0$ the BEC get a kick due to quenching of the potential and it starts moving towards the attractive Gaussian well. In Fig. 1 and Fig. 2, we can see that, for an attractive Gaussian well, $V_0 = -500$ and $V_0 = -1000$, respectively, in the absence of PT -symmetric environment, the analytical and numerical results match over a wide range of Gaussian well depths. In Fig. 1, we find out that the numerical and analytical results agree in the absence of PT -symmetric potential, Fig. 1(a-b), i.e., $W_0 = 0$, and in the presence of PT -symmetric potential, Fig. 1(c-d), i.e., $W_0 = 1$, very well with each other for $V_0 = -500$. Later, we plot Fig. 2 for a very high attractive Gaussian well, $V_0 = -1000$, where analytical and numerical results are matches in the absence Fig. 2(a-b), i.e., $W_0 = 0$ and mismatches in the presence of PT -symmetry Fig. 2(c-d), i.e., $W_0 = 1$. We note that the complex Ginzburg-Landau Eq. 6 valid for a large range of attractive Gaussian barriers well in the absence of PT -symmetric environment. However, CGLE Eq. 6 could not capture the physics of scattering of a BEC from an attractive Gaussian well in the presence of PT -symmetry for $W_0 \geq 1$.

B. Low Repulsive Gaussian Barrier

For a low repulsive barrier i.e., $V_0 = 100$, and in the absence of PT -symmetric environment, we compare analytical and numerical results in Fig. 3(a-b). While in Fig. 3(c-d), we show results in the presence of PT -symmetric environment both numerical and analytical. We note in Fig. 3(a,b) for a low barrier height, both the numerical and analytical results agree with each other. We find no discrepancy for the temporal density plot in Fig. 3(c-d), where the complex potential strength is $W_0 = 0.1$. Therefore, we can safely conclude that for a low repulsive Gaussian barrier, the complex-Ginsburg-Landau Eq. (6) capture the physics of scattering of a BEC, for a weak PT -symmetric potential.

C. High Repulsive Gaussian Barrier

In this subsection, we compare the analytical and numerical results for the scattering of a BEC from a high repulsive Gaussian barrier $V_0 = 500$. The analytic and numerical results are shown in Fig. 4(a,b) and Fig. 4(c,d) in

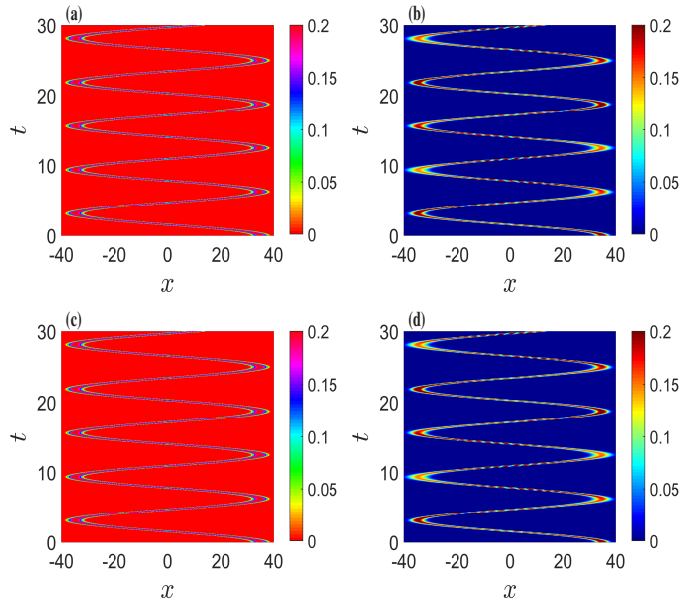


FIG. 1: (Color online) Numerical (left column) and analytical (middle column) density profile of the BEC scattering from an attractive Gaussian well $V_0 = -500$. The dimensionless parameters are, $g_s = 30$, and $x_0 = 35$. The Fig. (a,b) are the cases without PT -symmetric potential $W_0 = 0$, while for Fig. (c,d) the PT -symmetric potential is $W_0 = 1$. While the (right column) describes the time dependence of the mean-position and the width of the BEC wave-function.

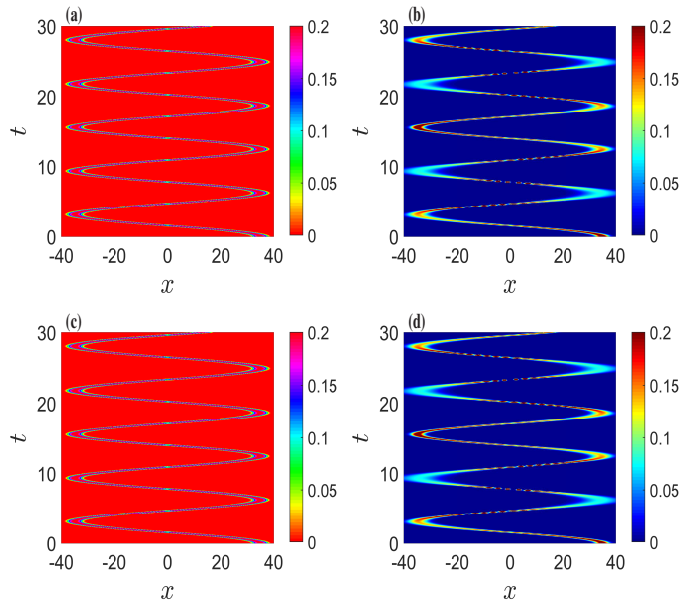


FIG. 2: (Color online) Comparison of numerical (left column) and analytical (right column) results for the scattering of a BEC from an attractive Gaussian well $V_0 = -1000$. The dimensionless parameters are, interaction strength $g_s = 30$, BEC is initially placed at $x_0 = 35$. The Fig. (a) and (b) are the cases without PT -symmetric potential. While for Fig (c) and (d) the dimensionless strength of the PT -symmetric potential is $W_0 = 1$.

the absence and in the presence of PT -symmetry potential environment respectively. We realize that the analytical results mismatch with the numerical simulations, as presented in Fig. 4. The reason for such a mismatch and the limitations of analytical results lies in the choice of the ansatz in Eq. (4). The initial ansatz, a Gaussian, deforms its shape during the collision with repulsive Gaussian barrier. We notice that higher the barrier, larger the deformation and hence larger is the mismatch. To get a good analytical result one needs a good ansatz with large ensemble of variational parameters. Such a large ensemble can make the problem cumbersome and notoriously complicated.

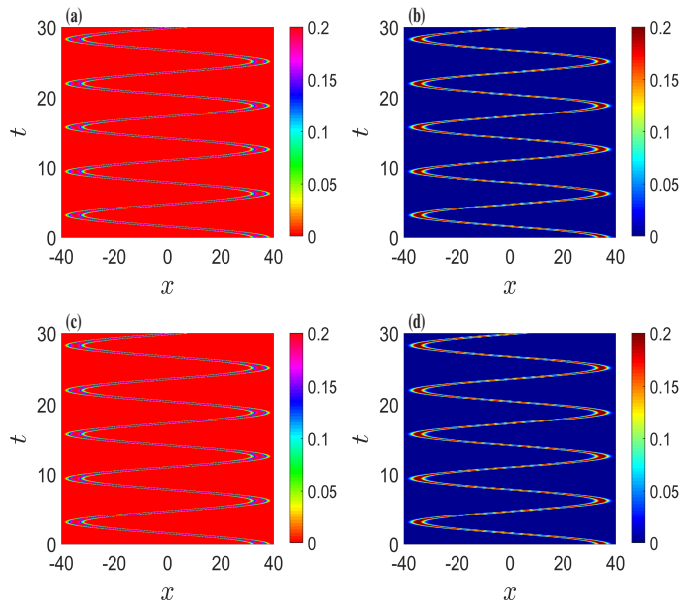


FIG. 3: (Color online) Comparison of numerical (left column) and analytical (right column) results for the scattering of a BEC from a low repulsive Gaussian barrier $V_0 = 100$. The dimensionless parameters are, interaction strength $g_s = 30$, BEC is initially placed at $x_0 = 35$. The Fig. (a) and (b) are the cases without PT -symmetric potential. While for Fig. (c) and (d) the dimensionless strength of the PT -symmetric potential is $W_0 = 0.1$.

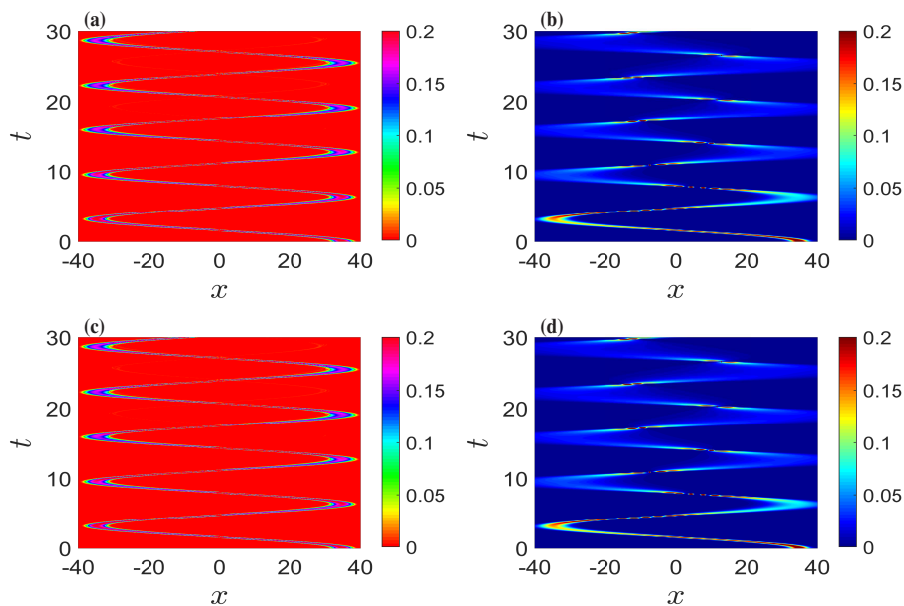


FIG. 4: (Color online) Comparison of numerical (left column) and analytical (right column) results for the scattering of a BEC from a large repulsive Gaussian barrier $V_0 = 500$. The dimensionless parameters are, interaction strength $g_s = 30$, BEC is initially placed at $x_0 = 35$. The Fig. (a) and (b) are the cases without PT -symmetric potential. While for Fig. (c) and (d) the dimensionless strength of the PT -symmetric potential is $W_0 = 0.1$.

Moreover, the collision of a BEC with the barrier generates the quasi-particles on the surface of the BEC, which makes it more hard for analytical analysis. Therefore, for the high repulsive Gaussian barrier more than $V_0 = 500$, the analytic results appears to lose the credibility. In our case, analytic results have limitations, it loses the true picture behind the physics of scattering of the BEC from the repulsive Gaussian barrier. Thus, from now on for the rest of this paper, we will rely only on our numerical simulations.

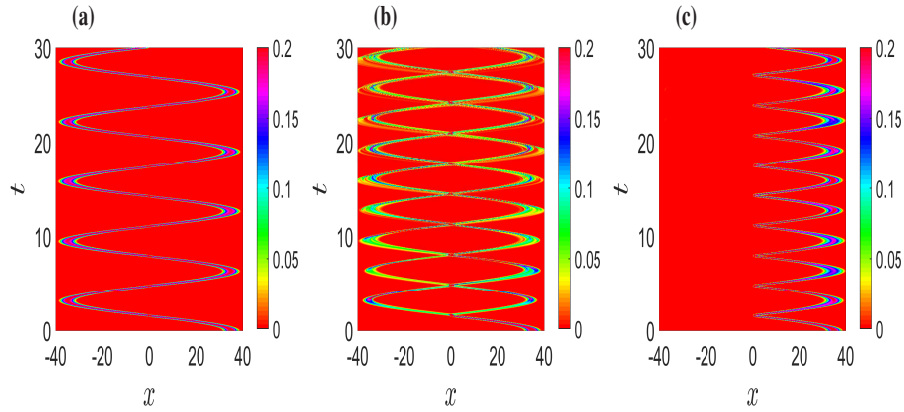


FIG. 5: (Color online) Numerically obtained temporal density graph shows the scattering of a BEC, in the absence of PT -Symmetric potential with dimensionless parameters $g_s = 30$, and $x_0 = 35$, from different repulsive barrier heights (a) $V_0 = 400$, (b) $V_0 = 600$, and (c) $V_0 = 700$.

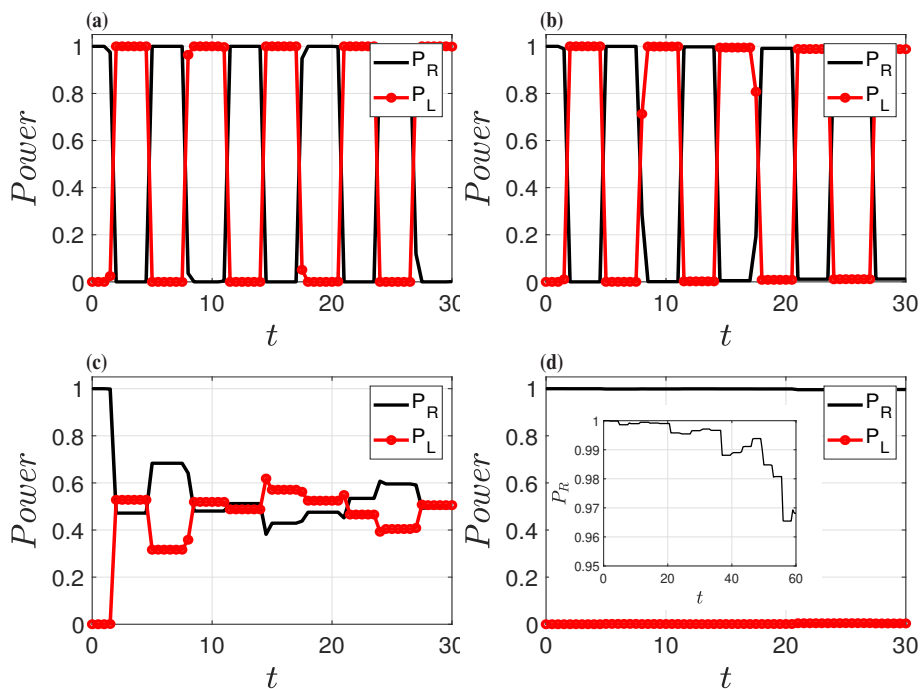


FIG. 6: (Color online) Power of a BEC versus the dimensionless time. The dimensionless parameters are $x_0 = 35$, $g_s = 30$ and Gaussian barrier heights are (a) $V_0 = 400$, (b) $V_0 = 500$, (c) $V_0 = 600$, and (d) $V_0 = 700$. The inset showing the decrease of a right side power (P_R) of the BEC with respect to time.

IV. NUMERICAL RESULTS IN THE ABSENCE OF PT -SYMMETRIC POTENTIAL

In this section, we discuss numerical results of a BEC scattering from a mild, high and very-high repulsive barrier for a conservative system, i.e., in the absence of PT -symmetric environment as shown in Fig. 5. In Fig. 5(a) and Fig. 4(a), we plot the temporal density graph of the BEC for the barrier heights $V_0 = 400$ and $V_0 = 500$, respectively. For these barrier heights the BEC unable to see the low barriers at all. The BEC does not see these barrier heights. Apparently the BEC experiences a harmonic confinement and performs to-and-fro motion. In Fig. 5(c) for high Gaussian potential barrier $V_0 = 600$, the BEC exhibit scattering, here, we observe reflection and transmission of the BEC at the barrier. In Fig. 5(d) for a very-high barrier height $V_0 = 700$ the BEC shows total reflection. Hence, the BEC is confined to the same side of the double well potential, where it was placed initially. This happen due to the very-high barrier height, however, one can observe a small tunneling of the BEC for a comparable large time. To

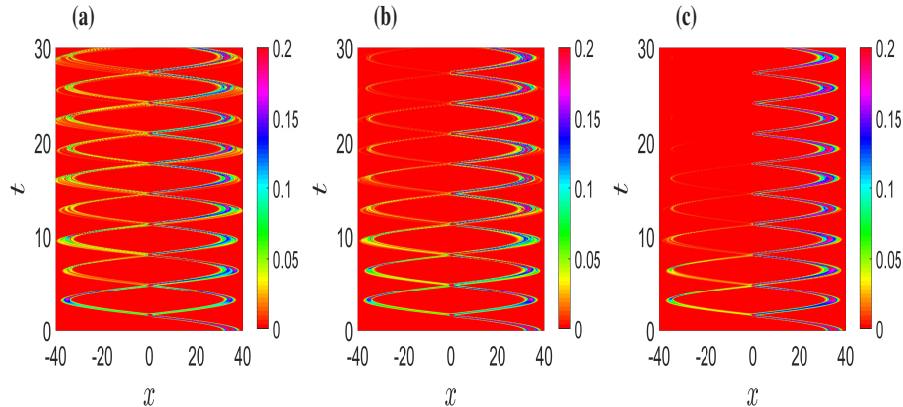


FIG. 7: (Color online) Numerically obtained temporal density graph shows the scattering of a BEC, in the presence of PT -Symmetric potential (a) $W_0 = 1$, (b) $W_0 = 5$, and (c) $W_0 = 10$ and other parameters are $V_0 = 600$, $g_s = 30$, and $x_0 = 35$.

quantify, this information, we plot the power of the BEC for the *Right* and the *Left* side of the Gaussian barrier. Here the *Left* side power (LSP) is defined as $P_L = \int_{-\infty}^0 |\psi|^2 dx$ and the *Right* side power (RSP) is represented as $P_R = \int_0^{\infty} |\psi|^2 dx$. Both powers RSP and LSP, fluctuate between “1” and “0”. We see from Fig. 6(a) that the initially BEC start moving towards the barrier from right side of the external potential. Therefore, initially the P_R starts from its maximum value “1” and P_L begins from “0”. However, as BEC moves in time, the power of the wavefunction start oscillating between P_L and P_R as shown in Fig. 6(a). Nevertheless, as we increase the barrier height from $V_0 = 500$ to $V_0 = 600$, we observe that the P_L and P_R starts oscillating. We also observe that both P_L and P_R tends to converge to 0.5, which shows presence of transmission and reflection of the BEC from the barrier, as shown in Fig. 6(c) and BEC is divided into two fragments as already depicted in Fig. 5(c). For $V_0 = 700$, the *Right* side power, P_R , of the BEC remains towards the *Right* side of the external potential, where it was trapped earlier. That is a clear sign of the confinement of a BEC on one side of the external Gaussian barrier potential. However, we also observe for a large dimensionless time, $t > 20$, a small amount of BEC tunnel through the barrier, which is a quantum mechanical effect, it can be made more visible by increasing the simulation time as shown in subset of Fig. 6(d).

V. NUMERICAL RESULTS IN THE PRESENCE OF PT -SYMMETRIC POTENTIAL

In this section, we discuss the numerical results of scattering of a BEC from a repulsive Gaussian barrier under a PT -symmetric environment as shown in Fig. 7. The Fig. 7(a-c) shows that the scattering of a BEC has been greatly influenced by the presence of loss and gain. Here the right side ($x > 0$) of the PT -symmetric potential represents the gain and the left side ($x < 0$) describes the loss in the system. Fig. 5(b) shows that the BEC is divided into two fragments for a barrier height of $V_0 = 600$ for $W_0 = 0$. The Fig. 7(a-c) for $W_0 = 1$, $W_0 = 5$ and $W_0 = 10$ reveals that the presence of loss and gain environment changes the reflection and transmission amount of the BEC considerably. Scattering of the BEC can be made more visible by plotting the *Left* side power, P_L and *Right* side power, P_R of the BEC as shown in Fig. 8(a-d). Here, we find out that as we increase the PT -Symmetric potential “ W_0 ”, the P_R starts growing with time. For example, for a specific case, Fig. 8(c) for $W_0 = 5$, we note that initially the P_R starts decreasing due to the BEC’s multiple reflections from the Gaussian barrier but gradually the amount of P_R rises as time goes on. Thus the PT -symmetric potential influence the transmission and tunneling of a BEC. We also observe in Fig. 8(d), that by increasing the amount of PT -symmetric potential $W_0 = 10$, the BEC stops penetrating into the left side of the potential from very early time as compared with the same potential barrier height. We also note that as time goes on the transmission of the BEC halt. Hence the P_R gradually grows to “1” and P_L decreases to “0”. We can safely say that the presence of the PT -symmetric potential turns the system into a unidirectional medium. The term “unidirectional” means that, we can control the direction of the transmission and tunneling of a BEC through a Gaussian barrier in the presence of PT -symmetric potential. Hence tuning to a specific reflection or transmission coefficient is possible through the external PT -symmetric potential. By using our technique, it also seems possible that one can calibrate the system for a specific amount of transmission/reflection for a desire time by just controlling the PT -symmetric potential.

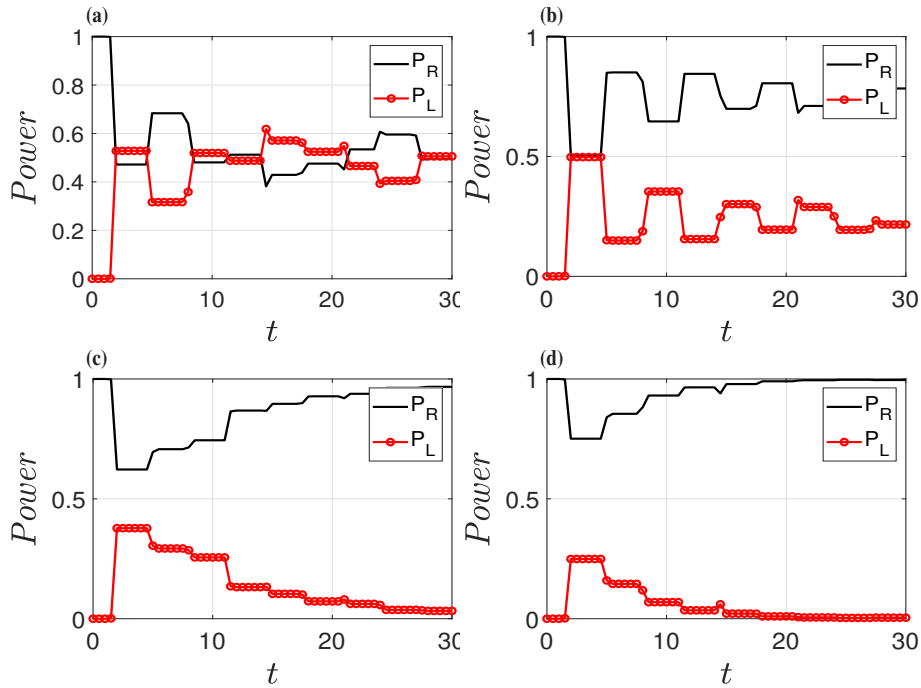


FIG. 8: (Color online) Power of a BEC under a PT -symmetric environment. The amount of dimensionless PT -symmetry potentials are (a) $W_0 = 0$, (b) $W_0 = 1$, (c) $W_0 = 5$ and (d) $W_0 = 10$. Other dimensionless parameter are $x_0 = 35$, $g_s = 30$ and $V_0 = 600$.

VI. CONCLUSION

In this paper, we study the impact of the presence of a PT -symmetric potential on the BEC transmission and reflections from a Gaussian well and Gaussian barrier. We find that scattering from the Gaussian barrier can be controlled by a combination of the barrier height and a PT -symmetric potential. In the first part of this research paper, we compare numerical simulation results with the analytical results obtained by using the Complex Ginzburg-Landau equation. We conclude that the CGLE captures the physics of the scattering of a BEC from a Gaussian well and from a low Gaussian barrier. However, the analytical results fail to capture the physics of the BEC scattering if a small amount of PT -symmetry, $W_0 > 0.1$, is present. We observe that the transmission and reflection at the barrier can be tuned by choosing a proper amount of PT -symmetry potential. In transistors, the "base" terminal controls the current through emitter and collector. Here, in our case, such PT -symmetric potentials control the transmission of the BEC in such a way that it behaves like a transistor, where the complex part of the potential serves like a "base". Moreover, our proposed model can be used as an atomic beam-splitter, in our proposed study by controlling the height of the barrier we can divide the density of the atomic beam into two parts for the varying density size. Additionally, by controlling the PT -symmetric strength, we can steer atomic beam-splitter density with respect to time, which can be seen as an additional feature of an atomic beam-splitter.

VII. ACKNOWLEDGMENT

Jameel Hussain gratefully acknowledges support from the COMSATS University Islamabad for providing him a workspace.

VIII. APPENDIX A

A complete solution for the Mean position of the BEC including "non-conservative" part of the Lagrangian

$$\begin{aligned}
x_0'' + x_0 = & \frac{2V_0x_0e^{-\frac{x_0^2}{\zeta}}}{\zeta^{3/2}} + \frac{W_0^2x_0(a^4+a^2+2x_0^2)(2a^6+a^4+(4a^2+2)x_0^2-a^2)e^{-\frac{2x_0^2}{\zeta}}}{a^2\zeta^6} \\
& + \frac{W_0e^{-\frac{x_0^2}{\zeta}}}{a\zeta^{9/2}} \left[2a\zeta x_0 (-a^4 + a^2 - 2x_0^2 + 2) x_0' \right. \\
& \left. + a' (3a^2\zeta^2 + 4a^2x_0^4 + 2(a^4 - 4a^2 + 1)\zeta x_0^2) \right]
\end{aligned} \tag{9}$$

Here, to write above equation into compact form we used these definitions $x_0 \equiv x_0(t)$, $a \equiv a(t)$. Width of the BEC including "non-conservative" part

$$\begin{aligned}
& \frac{2W_0^2x_0^2(2a^6+a^4+(4a^2+2)x_0^2-a^2)^2e^{-\frac{x_0^2}{\zeta}}}{a\sqrt{\zeta}} + \\
& + 2a\zeta W_0(ax_0a'((8a^2+4)x_0^4+(-2a^4+11a^2-2)\zeta^2+2(2a^4-11a^2-3)\zeta x_0^2) \\
& + \zeta(2a^8+3a^6-4(2a^2+1)x_0^4-a^2+(-4a^6+10a^4+20a^2+6)x_0^2)x_0') \\
& - 4a^3\zeta^4V_0(\zeta-2x_0^2) = -2a^2\zeta^{13/2}e^{\frac{x_0^2}{\zeta}} \left(-\frac{1}{a^3} - \frac{g_s}{\sqrt{2\pi}a^2} + a'' + a \right)
\end{aligned} \tag{10}$$

We solve these two coupled differential equations by using Mathematica command *NDSolve*. *NDSolve* commonly solves differential equations by using the Implicit-Runge-Kutta method or Explicit-Runge-Kutta method, depending on the type of equations. Indeed, both coupled differential equations are harder to solve, therefore, it is recommended to solve GPE numerically.

IX. REFERENCES

-
- * Electronic address: javedakram@daad-alumni.de
- [1] R. Clark, *Einstein: The Life and Times*, Discus books, HarperCollins, 1984.
URL <https://books.google.com.pk/books?id=6IKVA01Y6MAC>
 - [2] M. H. Anderson, J. R. Ensher, M. R. Matthews, C. E. Wieman, E. A. Cornell, Observation of Bose-Einstein Condensation in a Dilute Atomic Vapor, *Science* 269 (1995) 198. doi:10.1126/science.269.5221.198.
 - [3] K. B. Davis, M. O. Mewes, M. R. Andrews, N. J. van Druten, D. S. Durfee, D. M. Kurn, W. Ketterle, *Bose-Einstein Condensation in a Gas of Sodium Atoms*, *Phys. Rev. Lett.* 75 (1995) 3969–3973.
URL <http://link.aps.org/doi/10.1103/PhysRevLett.75.3969>
 - [4] L. Salasnich, A. Parola, L. Reatto, *Bose condensate in a double-well trap: Ground state and elementary excitations*, *Phys. Rev. A* 60 (1999) 4171–4174. doi:10.1103/PhysRevA.60.4171.
URL <https://link.aps.org/doi/10.1103/PhysRevA.60.4171>
 - [5] Y. Shin, C. Sanner, G.-B. Jo, T. A. Pasquini, M. Saba, W. Ketterle, D. E. Pritchard, M. Vengalattore, M. Prentiss, *Interference of bose-einstein condensates split with an atom chip*, *Phys. Rev. A* 72 (2005) 021604. doi:10.1103/PhysRevA.72.021604.
URL <https://link.aps.org/doi/10.1103/PhysRevA.72.021604>
 - [6] S. Middelkamp, G. Theocharis, P. G. Kevrekidis, D. J. Frantzeskakis, P. Schmelcher, *Dark solitons in cigar-shaped bose-einstein condensates in double-well potentials*, *Phys. Rev. A* 81 (2010) 053618. doi:10.1103/PhysRevA.81.053618.
URL <https://link.aps.org/doi/10.1103/PhysRevA.81.053618>
 - [7] J. Akram, A. Pelster, *Sculpting quasi-one-dimensional bose-einstein condensate to generate calibrated matter waves*, *Phys. Rev. A* 93 (2016) 023606. doi:10.1103/PhysRevA.93.023606.
URL <https://link.aps.org/doi/10.1103/PhysRevA.93.023606>
 - [8] J. Akram, A. Pelster, *Statics and dynamics of quasi one-dimensional bose-einstein condensate in harmonic and dimple trap*, *Laser Physics* 26 (6) (2016) 065501. doi:10.1088/1054-660x/26/6/065501.
URL <https://doi.org/10.1088/2F1054-660x/2F26/2F6/2F065501>
 - [9] A. M. Martin, R. G. Scott, T. M. Fromhold, *Transmission and reflection of bose-einstein condensates incident on a gaussian tunnel barrier*, *Phys. Rev. A* 75 (2007) 065602. doi:10.1103/PhysRevA.75.065602.
URL <https://link.aps.org/doi/10.1103/PhysRevA.75.065602>

- [10] V. J. Bolsinger, S. Krönke, P. Schmelcher, [Ultracold bosonic scattering dynamics off a repulsive barrier: Coherence loss at the dimensional crossover](#), Phys. Rev. A 96 (2017) 013618. doi:10.1103/PhysRevA.96.013618.
URL <https://link.aps.org/doi/10.1103/PhysRevA.96.013618>
- [11] J. Hussain, J. Akram, F. Saif, [Gray and dark soliton behavior and population under a symmetric and asymmetric potential trap](#), Journal of Low Temperature Physics 195 (5) (2019) 429–436. doi:10.1007/s10909-019-02172-z.
URL <https://doi.org/10.1007/s10909-019-02172-z>
- [12] P. Manju, K. S. Hardman, M. A. Sooriyabandara, P. B. Wigley, J. D. Close, N. P. Robins, M. R. Hush, S. S. Szigeti, [Quantum tunneling dynamics of an interacting bose-einstein condensate through a gaussian barrier](#), Phys. Rev. A 98 (2018) 053629. doi:10.1103/PhysRevA.98.053629.
URL <https://link.aps.org/doi/10.1103/PhysRevA.98.053629>
- [13] J. Akram, A. Pelster, [Numerical study of localized impurity in a bose-einstein condensate](#), Phys. Rev. A 93 (2016) 033610. doi:10.1103/PhysRevA.93.033610.
URL <https://link.aps.org/doi/10.1103/PhysRevA.93.033610>
- [14] J. Akram, [A distinguishable single excited-impurity in a bose-einstein condensate](#), Laser Physics Letters 15 (2) (2018) 025501. doi:10.1088/1612-202x/aa8ec4.
URL <https://doi.org/10.1088/1612-202x/aa8ec4>
- [15] C. M. Bender, S. Boettcher, [Real spectra in non-hermitian hamiltonians having \$pt\$ symmetry](#), Phys. Rev. Lett. 80 (1998) 5243–5246. doi:10.1103/PhysRevLett.80.5243.
URL <https://link.aps.org/doi/10.1103/PhysRevLett.80.5243>
- [16] C. M. Bender, [Pt symmetry in quantum physics: From a mathematical curiosity to optical experiments](#), Europhysics News 47 (2) (2016) 17–20. doi:10.1051/epn/2016201.
URL <https://doi.org/10.1051/epn/2016201>
- [17] R. El-Ganainy, K. G. Makris, D. N. Christodoulides, Z. H. Musslimani, [Theory of coupled optical \$pt\$ -symmetric structures](#), Opt. Lett. 32 (17) (2007) 2632–2634. doi:10.1364/OL.32.002632.
URL <http://ol.osa.org/abstract.cfm?URI=ol-32-17-2632>
- [18] A. Ruschhaupt, F. Delgado, J. G. Muga, [Physical realization of \$\mathcal{P}\$ -symmetric potential scattering in a planar slab waveguide](#), Journal of Physics A: Mathematical and General 38 (9) (2005) L171–L176. doi:10.1088/0305-4470/38/9/L03.
URL <https://doi.org/10.1088/0305-4470/38/9/L03>
- [19] F. S. Y. Christodoulides, Demetrios N.; Lederer, [Discretizing light behaviour in linear and nonlinear waveguide lattices](#), Nature 424 (2003) 817–823. doi:10.1038/nature01936.
URL <http://gen.lib.rus.ec/scimag/10.1038/nature01936>
- [20] E. M. Graefe, H. J. Korsch, A. E. Niederle, [Mean-field dynamics of a non-hermitian bose-hubbard dimer](#), Phys. Rev. Lett. 101 (2008) 150408. doi:10.1103/PhysRevLett.101.150408.
URL <https://link.aps.org/doi/10.1103/PhysRevLett.101.150408>
- [21] E.-M. Graefe, H. J. Korsch, A. E. Niederle, [Quantum-classical correspondence for a non-hermitian bose-hubbard dimer](#), Phys. Rev. A 82 (2010) 013629. doi:10.1103/PhysRevA.82.013629.
URL <https://link.aps.org/doi/10.1103/PhysRevA.82.013629>
- [22] S. Klaiman, U. Günther, N. Moiseyev, [Visualization of branch points in \$\mathcal{PT}\$ -symmetric waveguides](#), Phys. Rev. Lett. 101 (2008) 080402. doi:10.1103/PhysRevLett.101.080402.
URL <https://link.aps.org/doi/10.1103/PhysRevLett.101.080402>
- [23] G. Barontini, R. Labouvie, F. Stubenrauch, A. Vogler, V. Guarrera, H. Ott, [Controlling the dynamics of an open many-body quantum system with localized dissipation](#), Phys. Rev. Lett. 110 (2013) 035302. doi:10.1103/PhysRevLett.110.035302.
URL <https://link.aps.org/doi/10.1103/PhysRevLett.110.035302>
- [24] T. Gericke, P. Wurtz, D. Reitz, T. Langen, H. Ott, [High-resolution scanning electron microscopy of an ultracold quantum gas](#), Nature Physics 4 (2008) 949. doi:10.1038/nphys1102.
URL <http://doi.org/10.1038/nphys1102>
- [25] J. I. Cirac, M. Lewenstein, P. Zoller, [Collective laser cooling of trapped atoms](#), Europhysics Letters (EPL) 35 (9) (1996) 647–652. doi:10.1209/epl/i1996-00165-4.
URL <https://doi.org/10.1209/epl/i1996-00165-4>
- [26] P. D. J. C. J. Robins, N.P.; Altin, [Atom lasers: Production, properties and prospects for precision inertial measurement](#), Physics Reports 529 (2013) 265–296. doi:10.1016/j.physrep.2013.03.006.
URL <http://doi.org/10.1016/j.physrep.2013.03.006>
- [27] M. Kreibich, J. Main, H. Cartarius, G. Wunner, [Hermitian four-well potential as a realization of a \$\mathcal{PT}\$ -symmetric system](#), Phys. Rev. A 87 (2013) 051601. doi:10.1103/PhysRevA.87.051601.
URL <https://link.aps.org/doi/10.1103/PhysRevA.87.051601>
- [28] M. Olshanii, [Atomic scattering in the presence of an external confinement and a gas of impenetrable bosons](#), Phys. Rev. Lett. 81 (1998) 938–941. doi:10.1103/PhysRevLett.81.938.
URL <https://link.aps.org/doi/10.1103/PhysRevLett.81.938>
- [29] D. Petrov, D. Gangardt, G. V. Shlyapnikov, [Low-dimensional trapped gases](#), Journal de Physique IV 116 (2004) 5–44. doi:10.1051/jp4:2004116001.
URL <http://doi.org/10.1051/jp4/3A2004116001>
- [30] E. P. Gross, [Hydrodynamics of a Superfluid Condensate](#), Journal of Mathematical Physics 4 (1963) 195. doi:10.1063/1.1703944.
- [31] L. P. Pitaevsk, [VORTEX LINES IN AN IMPERFECT BOSE GAS](#), Soviet Physics JETP-USSR 13 (1961) 2.

- [32] D. Anderson, *Variational approach to nonlinear pulse propagation in optical fibers*, Phys. Rev. A 27 (1983) 3135–3145. doi:10.1103/PhysRevA.27.3135.
URL <https://link.aps.org/doi/10.1103/PhysRevA.27.3135>
- [33] V. M. Pérez-García, H. Michinel, J. I. Cirac, M. Lewenstein, P. Zoller, *Dynamics of bose-einstein condensates: Variational solutions of the gross-pitaevskii equations*, Phys. Rev. A 56 (1997) 1424–1432. doi:10.1103/PhysRevA.56.1424.
URL <https://link.aps.org/doi/10.1103/PhysRevA.56.1424>
- [34] Chávez Cerda, S., Cavalcanti, S. B., Hickmann, J. M., *A variational approach of nonlinear dissipative pulse propagation*, Eur. Phys. J. D 1 (3) (1998) 313–316. doi:10.1007/s100530050098.
URL <https://doi.org/10.1007/s100530050098>
- [35] A. Ankiewicz, N. Akhmediev, N. Devine, *Dissipative solitons with a lagrangian approach*, Optical Fiber Technology 13 (2007) 91–97. doi:10.1016/j.yofte.2006.12.001.
URL <http://doi.org/10.1016/j.yofte.2006.12.001>
- [36] L. Devassy, C. P. Jisha, A. Alberucci, V. C. Kuriakose, *Parity-time-symmetric solitons in trapped bose-einstein condensates and the influence of varying complex potentials: A variational approach*, Phys. Rev. E 92 (2015) 022914. doi:10.1103/PhysRevE.92.022914.
URL <https://link.aps.org/doi/10.1103/PhysRevE.92.022914>
- [37] S. Hu, H. Chen, W. Hu, *A variational solution to solitons in parity-time symmetric optical lattices*, The European Physical Journal Plus 132 (2017) 374. doi:10.1140/epjp/i2017-11611-9.
URL <http://doi.org/10.1140/epjp%2Fi2017-11611-9>
- [38] W. Bao, D. Jaksch, P. A. Markowich, *Numerical solution of the Gross–Pitaevskii equation for Bose–Einstein condensation*, Journal of Computational Physics 187 (1) (2003) 318–342. doi:10.1016/S0021-9991(03)00102-5.
URL <http://www.sciencedirect.com/science/article/pii/S0021999103001025>
- [39] D. Vudragović, I. Vidanović, A. Balaž, P. Muruganandam, S. K. Adhikari, *C programs for solving the time-dependent Gross–Pitaevskii equation in a fully anisotropic trap*, Comp. Phys. Commun. 183 (9) (2012) 2021–2025. doi:10.1016/j.cpc.2012.03.022.
URL <http://www.sciencedirect.com/science/article/pii/S0010465512001270>
- [40] R. K. Kumar, L. E. Young-S., D. Vudragović, A. Balaž, P. Muruganandam, S. Adhikari, *Fortran and C programs for the time-dependent dipolar Gross–Pitaevskii equation in an anisotropic trap*, Comput. Phys. Commun. 195 (2015) 117–128. doi:10.1016/j.cpc.2015.03.024.
- [41] V. Lončar, A. Balaž, A. Bogojević, S. Škrbić, P. Muruganandam, S. K. Adhikari, *CUDA programs for solving the time-dependent dipolar Gross–Pitaevskii equation in an anisotropic trap*, Comput. Phys. Commun. 200 (2016) 406. doi:10.1016/j.cpc.2015.11.014.
- [42] B. Satarić, V. Slavnić, A. Belić, A. Balaž, P. Muruganandam, S. K. Adhikari, *Hybrid OpenMP/MPI programs for solving the time-dependent Gross–Pitaevskii equation in a fully anisotropic trap*, Comput. Phys. Commun. 200 (2016) 411. doi:10.1016/j.cpc.2015.12.006.
URL <http://www.sciencedirect.com/science/article/pii/S0010465515004440>
- [43] C. Zhu, L. Dong, H. Pu, *Harmonically trapped atoms with spin–orbit coupling*, Journal of Physics B: Atomic, Molecular and Optical Physics 49 (14) (2016) 145301. doi:10.1088/0953-4075/49/14/145301.
URL <https://doi.org/10.1088%2F0953-4075%2F49%2F14%2F145301>